

## Biological cell as a soft magnetoelectric material: Elucidating the physical mechanisms underpinning the detection of magnetic fields by animals

S. Krichen,<sup>1</sup> L. Liu,<sup>2,\*</sup> and P. Sharma<sup>1,3,†</sup><sup>1</sup>*Department of Mechanical Engineering, University of Houston, Houston, Texas 77204, USA*<sup>2</sup>*Department of Mathematics and Department of Mechanical Aerospace Engineering, Rutgers University, Piscataway, New Jersey 08854, USA*<sup>3</sup>*Department of Physics, University of Houston, Houston, Texas 77204, USA*

(Received 4 July 2016; revised manuscript received 19 July 2017; published 4 October 2017)

Sharks, birds, bats, turtles, and many other animals can detect magnetic fields. Aside from using this remarkable ability to exploit the terrestrial magnetic field map to sense direction, a subset is also able to implement a version of the so-called geophysical positioning system. How do these animals detect magnetic fields? The answer to this rather deceptively simple question has proven to be quite elusive. The currently prevalent theories, while providing interesting insights, fall short of explaining several aspects of magnetoreception. For example, minute magnetic particles have been detected in magnetically sensitive animals. However, how is the detected magnetic field converted into electrical signals given any lack of experimental evidence for relevant electroreceptors? In principle, a magnetoelectric material is capable of converting magnetic signals into electricity (and vice versa). This property, however, is rare and restricted to a rather small set of exotic hard crystalline materials. Indeed, such elements have never been detected in the animals studied so far. In this work we quantitatively outline the conditions under which a biological cell may detect a magnetic field and convert it into electrical signals detectable by biological cells. Specifically, we prove the existence of an overlooked strain-mediated mechanism and show that most biological cells can act as nontrivial magnetoelectric materials provided that the magnetic permeability constant is only slightly more than that of a vacuum. The enhanced magnetic permeability is easily achieved by small amounts of magnetic particles that have been experimentally detected in magnetosensitive animals. Our proposed mechanism appears to explain most of the experimental observations related to the physical basis of magnetoreception.

DOI: [10.1103/PhysRevE.96.042404](https://doi.org/10.1103/PhysRevE.96.042404)

### I. INTRODUCTION

An astonishing number of animals exhibit the ability to detect magnetic fields (see Refs. [1–4]). Examples (Fig. 1) include migratory birds, sea turtles, sharks, bats, lobsters, and many others. Experiments have well documented the ability of the aforementioned animals to exploit the terrestrial magnetic field to either obtain directional information [5–7] or, in a subset of these magnetically sensitive animals, even infer positional information [8–10]. The latter has been compared to having a low-resolution biological equivalent of the Geophysical Positioning System [11,12]. The central question pertaining to how precisely animals detect magnetic fields has attracted much attention over the years, but the mechanism underlying this ability remains controversial and arguably unresolved. An article by Lohmann [11] provides an excellent perspective on the open questions underlying this subject.

The detection of the so-called magnetoreceptors in animals is rather challenging. The action of the magnetic field is nonlocal and (ostensibly) biological tissue is essentially transparent to its effect. Furthermore, the pervasiveness of the weak geomagnetic field does not provide an option to switch off the field to facilitate the location of magnetoreceptors [13]. In other words, we have a little intuition about the existence of any organ that supports magnetoreception and as the magnetic sensory system is still unknown, identification of magnetoreceptors that might be made of a small number

of microscopic intracellular structures and located anywhere within the animal body has proven to be quite difficult.

Three key mechanisms have been proposed to explain the phenomenon of magnetoreception: electromagnetic induction, the presence of magnetite particles, and so-called chemical magnetoreception [5,11,14–21]. The idea of electromagnetic induction was suggested based on the presence of Lorenzini ampullae cells in a variety of aquatic saltwater fish such as sharks, skates, and rays. They work as highly sensitive electroreceptors. As the (electrically conductive) fish swim in a conductive media (seawater) through a stationary geomagnetic field, a nonuniform charge distribution across the fish's body is produced, thus forming a closed electric circuit. The induced current flowing through the circuit is detected by the electroreceptors. The magnetite-based hypothesis was suggested after the detection of iron oxide in animals sensitive to geomagnetism. Researchers have argued that upon exposure to a magnetic field, magnetites, while aligning themselves with respect to the field, may trigger other sensory structures that allow its detection [15,22–24]. Finally, a few researchers have argued in favor of a chemical origin for magnetoreception that involves how magnetic fields may influence certain chemical reactions at the cellular level [5,14,16–19,25–29].

The following observations may be made about the three aforementioned proposals that purport to explain magnetoreception in animals.

(i) The key shortcoming in the magnetic-induction-based proposed mechanism is that both the animal body and the ambient medium must be electrically conductive. While the induction mechanism may explain observations related to aquatic animals, this is decidedly not the case for land-based

\*Corresponding author: [liu.liping@rutgers.edu](mailto:liu.liping@rutgers.edu)†Corresponding author: [psharma@central.uh.edu](mailto:psharma@central.uh.edu)



FIG. 1. Magnetosensitive animals. Shown on top are European robins, which have an avian magnetic compass that has been extensively researched. Shown on the bottom are sharks, which are among the numerous marine animals that can perceive the Earth's magnetic field.

magnetosensitive animals that navigate in nonconductive air [30,31].

(ii) Iron oxide particles (magnetite) have indeed been discovered in some magnetically sensitive animals. For example, they were located within cells in the olfactory lamellae for trouts [32,33]. There is some controversy related to the findings of these particles in the upper beaks of pigeons [34–38]. In any case, according to the magnetite-dependent hypothesis, the cells of interest should respond to a change in the magnetic field. However, an explanation of how this leads to a conversion of magnetic field into electrical signals detectable by the nervous system remains anatomically unanswered.

(iii) The chemical magnetoreception mechanism, while physically well grounded, is criticized on the grounds that its central premise has only been experimentally confirmed for magnetic field intensities that far exceed the weak field of Earth [5]. We refer the reader to the paper by Hore and Mouritsen for a review [16]. An experimental proof of the principle underpinning this mechanism was provided in Ref. [39].

In principle, the presence of a certain class of materials in the animal bodies, called magnetoelectrics, would readily

explain magnetoreception. Such materials have the tantalizing ability to convert magnetic fields into electrical signals and vice versa. Indeed, there is intense research in the pursuit of several applications based on such materials e.g., wireless energy transfer [40], spintronics, multiple-state memory bits [41], and nonvolatile memories, among others [42]. However, single-phase magnetoelectric materials are rare and restricted to a small set of exotic hard crystalline materials. Certainly, there is no current scientific reason to believe that soft biological cells are capable of exhibiting this exotic effect that appears to be the sole feature of complex hard crystalline materials. Based on our recent work [43], we propose an overlooked strain-mediated mechanism that can be employed to universally induce a magnetoelectric effect in all (sufficiently) soft dielectric materials. In this work we establish the precise conditions under which a typical biological cell can act as a magnetoelectric material, i.e., convert magnetic signals into electrical ones. Our model appears to explain most of the key experimental observations related to the physical basis of magnetoreception and is arguably fairly simple in principle and (at least to the magnetite-based mechanism) complementary<sup>1</sup> in character. The last point is worth reiterating. Our proposed mechanism does not rule out the existing proposals but merely asserts that what our quantitative results (to be elaborated upon) provide is perhaps the most direct manner in which magnetic signals may be converted into electrical ones.

## II. PHYSICAL AND MATHEMATICAL MODEL

In this section we will establish the conditions under which a typical biological cell can act as a magnetoelectric material. Our central premise is that geometrically nonlinear (large) deformation and electromagnetism must be carefully accounted for to correctly yield the hypothesized electromagnetomechanical coupling. As will become evident in due course, considering these multiphysics-field couplings is essential to ensure that the mechanism we propose is adequately captured. The central physical idea is embodied in Fig. 2. The intracellular media, in the absence of a magnetic field, is considered to be of spherical shape and enclosed by a soft homogeneous dielectric thin lipid membrane. The assumption of this idealized shape is unimportant to the key results of our work. The membrane is assumed to be elastically nonlinear.

Consistent with what we know about biological cells, we assume that there is no intrinsic magnetoelectric coupling in the cell. Nevertheless, it is well known that cell membranes possess a cross-membrane resting potential difference due to

<sup>1</sup>We characterize our work as complementary since it, like other existing models, also presupposes the presence of magnetic particles but provides an explanation for how precisely this translates into the conversion of a magnetic signal to an electrical one. On this note, however, it is worth mentioning that Kirschvink and Gould have proposed a model based on the fact that magnetites are also good electrical conductors. It is speculated that under suitable conditions, magnetites may depolarize the membrane of a sensory organelle and thus alter the electric potential across it [24].

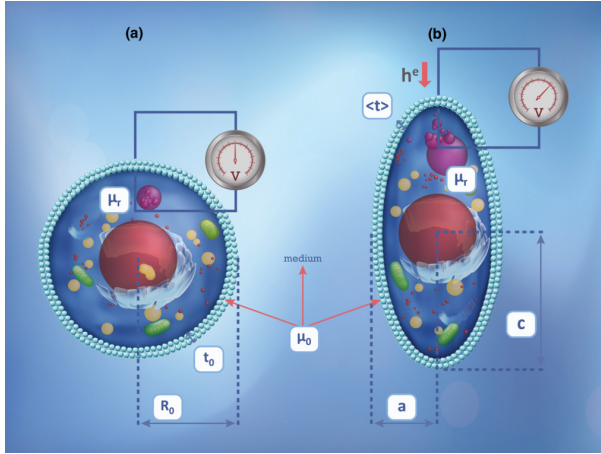


FIG. 2. Conceptual schematic of the magnetosensitive biological cell. The cell is enclosed by a soft homogeneous dielectric thin membrane of dielectric permittivity  $\epsilon_r$ , and we will assume that the permeability of the membrane and its surrounding is about the same as in a vacuum ( $\mu_r = 1$ ). However, the interior of the cell may have a different magnetic permeability  $\mu_r > 1$ . (a) The state where the cell is perfectly spherical is hypothetical but useful as a reference to explain the mechanism outlined in the text. (b) As is well known, we consider the cell membrane to possess a preexisting (or resting) voltage across its thickness. The electrical field due to the resting voltage leads to the so-called electrical Maxwell stress and polarizes the membrane. We assume that our starting configuration is a nearly spherical ellipsoid as discussed in the text. The magnetic field is now switched on. The magnetic Maxwell stress causes further deformation and consequently alters the preexisting electric field across the membrane.

actively regulated ion transportation (the typical value of this potential difference is around 50 mV) and hence a preexisting electric field in the membrane. We assume the initial configuration of the cell to be ellipsoidal (but nearly spherical).<sup>2</sup> This preexisting electric field will polarize the membrane and deform the overall cell via the electrical Maxwell stress, a well-known mechanical effect of the electromagnetic field since Maxwell [44]. In other words, due to the preexisting

<sup>2</sup>The initial configuration can be found by minimizing the electrostatic and elastic energy and solving the resulting nonlinear equations. The energy of the configuration as a function of the aspect ratio is nearly flat around 1. This implies that there are configurations that are very close to the sphere and the energy function has a double-well form. The sphere solution (i.e., aspect ratio equal to 1) is in fact metastable (even though the adjacent prolate and oblate ellipsoidal states differ very little in energy). Accordingly, in practice, even though our reference state is a sphere, any minor perturbation or fluctuation will inevitably break this symmetry and the sphere will immediately transform to an adjacent state corresponding to a prolate or an oblate ellipsoid. This is the reason we have chosen an ellipsoid as a starting point. We remark that the central idea discussed in the present work is insensitive to the initial configuration and the different physics pertains to how the configuration changes as a result of magnetic fields.

resting potential across the membrane, the biological cell is deformed and exhibits a residual electric field. Now imagine the action of an external magnetic field on this biological cell. What will be its effect? We will show shortly that under certain conditions (to be specified), the magnetic Maxwell stress (in analogy to the electric Maxwell stress) is nontrivial and will further deform the cell and change the thickness of the membrane. The thinning of the membrane will, due to the constant resting potential across the membrane, induce changes of electric field and polarization of the membrane and an overall electrical current (or transportation of ions) in the extracellular media. In other words, there will be a change in the preexisting electric field upon the action of the magnetic field; this is precisely the magnetoelectric effect.

Thus, in principle, the biological cell can act as a magnetoelectric material, i.e., it can convert magnetic signals into electric ones provided that (i) there is a preexisting electric field across the membrane, (ii) the magnetic Maxwell stress is nontrivial for the cell, and (iii) the membrane and biological cell are elastically soft enough that both electric and magnetic Maxwell stress can significantly deform them and therefore cause a detectable change in the electrical field. Items (i) and (iii) are readily met in typical biological cells (although we will quantify this as well). The insights into the second condition will emerge from our mathematical translation of the physical model of a dielectric elastic cell membrane separating conducting intracellular and extracellular fluids. To that end, we introduce an elastic membrane of relative dielectric permittivity  $\epsilon_r$  and magnetic permeability  $\mu_r = 1$  separating the cell interior from the outside (electrolytic) media. We assume that the exterior medium is conductive with relative magnetic permeability like that of a vacuum  $\mu_r = 1$ . Likewise, the interior medium of the cell is also assumed to be conductive, although we leave its magnetic permeability unspecified and denote it by  $\mu_r$ . Let  $\mathcal{M} \subset \mathbb{R}^3$  be the three-dimensional membrane body with midsurface being  $\partial\Omega$ . In a reference configuration when there is no magnetic field or potential difference, the membrane body  $\mathcal{M}_0$  is a shell of thickness  $t_0$  and inner radius  $R_0$  ( $t_0 \ll R_0$ ). Let  $\mathbf{y} : \mathcal{M}_0 \rightarrow \mathcal{M}$  be the deformation of the membrane with reference midsurface  $\partial\Omega_0$  and deformed midsurface  $\partial\Omega$ . We denote by  $\mathbf{p} : \mathcal{M} \rightarrow \mathbb{R}^3$  and  $\mathbf{m} : \Omega \rightarrow \mathbb{R}^3$ , respectively, the polarization in the membrane and the magnetization in the intracellular media in the deformed configuration that describes the thermodynamic state of the system. Since the central idea is related to nonlinear deformation state, the distinction between the reference and deformed configuration must be carefully maintained. Constitutively, we assume linear dielectric behavior of the membrane (of relative permittivity  $\epsilon_r$ ) and magnetic behavior of the intracellular fluid (of relative permeability  $\mu_r$ ):<sup>3</sup>

$$\begin{aligned} \mathbf{e} &= \frac{\mathbf{p}}{\epsilon_0(\epsilon_r - 1)} & \text{in } \mathcal{M}, \\ \mathbf{h} &= \frac{\mathbf{m}}{\mu_r - 1} & \text{in } \Omega, \end{aligned} \quad (1)$$

<sup>3</sup>The key nonlinearities that must be accounted for are geometric in nature and not constitutive.

where  $\mathbf{e}$  ( $\mathbf{h}$ ) denotes the spatial electric field (magnetic field) and  $\epsilon_0$  ( $\mu_0$ ) the vacuum electric permittivity (magnetic permeability). We are interested in how the external magnetic field  $\mathbf{h}^e$  influences the equilibrium state of the system and in particular the electric field across the cell membrane.

Under the application of a cross-membrane resting potential  $V_0$  and external magnetic field  $\mathbf{h}^e$ , the total free energy of the system can be identified as

$$F[\mathbf{y}, \mathbf{p}, \mathbf{m}; V_0, \mathbf{h}^e] = U_{\text{elast}}[\mathbf{y}] + \mathcal{E}_{\text{elct}}[\mathbf{y}, \mathbf{p}; V_0] + \mathcal{E}_{\text{mag}}[\mathbf{y}, \mathbf{m}; \mathbf{h}^e], \quad (2)$$

where  $U_{\text{elast}}$  is the elastic energy arising from the deformation of the elastic membrane and  $\mathcal{E}_{\text{elct}}$  ( $\mathcal{E}_{\text{mag}}$ ) is the electric (magnetic) contribution to the free energy. For simplicity, we make the assumption that the intracellular and extracellular media are fluids whose elasticity is negligible. The energy penalty associated with the thickness deformation and the stretching is used to describe the elastic behavior of the membrane

$$U_{\text{elast}}[\mathbf{y}] = \int_{\partial\Omega} \left[ \frac{\kappa_t}{2} \left( \frac{t}{t_0} - 1 \right)^2 \right] + \frac{\kappa_s}{2} \frac{(|\partial\Omega| - |\partial\Omega_0|)^2}{|\partial\Omega_0|}, \quad (3)$$

where  $\partial\Omega = \mathbf{y}(\partial\Omega_0)$ ,  $\kappa_t$  is the modulus associated with thickness changes and has units of energy per unit area,  $\kappa_s$  is the stretch modulus,  $t_0$  is the thickness in the reference configuration, and  $t$  is the thickness of the deformed membrane. The change in the bending energy is negligible in this context and hence ignored. In addition, since the biological membrane is essentially a fluid membrane, we assume that it is effectively incompressible. Therefore, we have

$$\mathcal{I}_1[\mathbf{y}] = \int_{\partial\Omega} t - \int_{\partial\Omega_0} t_0 = 0. \quad (4)$$

Furthermore, we assume that the cell volume remains constant during the deformation and hence we have

$$\mathcal{I}_2[\mathbf{y}] = \Delta\Omega = 0. \quad (5)$$

Also, the electric contribution to the free energy is identified as [51,52]

$$\mathcal{E}_{\text{elct}}[\mathbf{y}, \mathbf{p}; V_0] = \int_{\mathcal{M}} \frac{|\mathbf{p}|^2}{2\epsilon_0(\epsilon_r - 1)} + \frac{\epsilon_0}{2} \int_{\mathcal{M}} |\nabla\varphi|^2 + \int_{\partial\mathcal{M}} \varphi(-\epsilon_0\nabla\varphi + \mathbf{p}) \cdot \mathbf{n}, \quad (6)$$

where the electric potential  $\varphi : \mathcal{M} \rightarrow \mathbb{R}$  is determined by the Maxwell equation

$$\begin{aligned} \text{div}(-\epsilon_0\nabla\varphi + \mathbf{p}) &= 0 \quad \text{in } \mathcal{M}, \\ \varphi|_{\text{interior}} &= 0, \quad \varphi|_{\text{exterior}} = V_0. \end{aligned} \quad (7)$$

Finally, by the Landau theory of micromagnetics, the magnetic contribution to the free energy can be written as

$$\mathcal{E}_{\text{mag}}[\mathbf{y}, \mathbf{m}; \mathbf{h}^e] = \int_{\Omega} \frac{\mu_0}{2(\mu_r - 1)} |\mathbf{m}|^2 + \int_{\mathbb{R}^3} \left[ \frac{\mu_0}{2} |\nabla\xi|^2 - \mu_0 \mathbf{h}^e \cdot \mathbf{m} \right], \quad (8)$$

where the self magnetic potential  $\xi : \mathbb{R}^3 \rightarrow \mathbb{R}$  must also satisfy the Maxwell equation

$$\begin{aligned} \text{div}(-\nabla\xi + \mathbf{m}\chi_{\Omega}) &= 0 \quad \text{in } \mathbb{R}^3, \\ \xi &\rightarrow 0 \quad \text{as } |\mathbf{x}| \rightarrow +\infty, \end{aligned} \quad (9)$$

Here  $\chi_{\Omega} = 1$  on  $\Omega$  and 0 otherwise. The source term  $\mathbf{m}\chi_{\Omega}$  in Eq. (9) reflects that only the intracellular medium is magnetizable because of the enclosed nanoscale magnetic proteins or particles. In conclusion, the principle of minimum free energy asserts that the equilibrium state of the system is such that

$$\min\{F[\mathbf{y}, \mathbf{p}, \mathbf{m}; V_0, \mathbf{h}^e] : (\mathbf{y}, \mathbf{p}, \mathbf{m}) \in \mathcal{S}\}, \quad (10)$$

where  $\mathcal{S}$  represents the admissible space of the state variables  $(\mathbf{y}, \mathbf{p}, \mathbf{m})$ .

A few remarks are in order here concerning the thermodynamic theory for electromagnetomechanical coupling described in the previous paragraphs. First, as already mentioned, the postulated behavior of the system contains no intrinsic magnetoelectric coupling, i.e., there is no direct coupling term between  $\mathbf{p}$  and  $\mathbf{m}$  in the system free energy (2). Indeed, as may be readily observed by minimizing the free energy with respect to the polarization  $\mathbf{p}$  and magnetization  $\mathbf{m}$  (see details in Ref. [51]), the magnetic and electric behaviors of the system obey the usual uncoupled linear constitutive relations (1). However, a change of external magnetic field  $\mathbf{h}^e$  does induce a change of polarization  $\mathbf{p}$  in the membrane due to a nonlinear coupling via mechanical deformation, as can be discerned by the solution to the minimization problem in Eq. (10) and shown numerically in the next section.

In what follows, both for conceptual simplicity and to clearly distill the physical implications of our mathematical model, we solve the minimization problem in Eq. (10) predicated on two different assumptions related to the deformation of the cell membrane.

(i) As a first solution, we assume that the change in thickness of the deformed membrane  $\mathcal{M}$  is uniform ( $t = \bar{t} = \text{const}$  on  $\partial\Omega$ ) and the overall cell is deformed into a spheroid with semiaxis length  $(a, a, c)$  (the  $c$  axis is along the external magnetic field  $\mathbf{h}^e$  direction). Then, in terms of  $(a, c, \bar{t})$ , we can rewrite the free energy (2) as (see the Appendix)

$$\begin{aligned} F(a, c, \bar{t}) &= \frac{\kappa_t}{2} \left( \frac{\bar{t}}{t_0} - 1 \right)^2 |\partial\Omega| + \frac{\kappa_s}{2} \frac{(|\partial\Omega| - |\partial\Omega_0|)^2}{|\partial\Omega_0|} \\ &\quad - \frac{\epsilon_0\epsilon_r}{2} \left( \frac{V_0^2}{\bar{t}} \right) |\partial\Omega| - \frac{(\mu_r - 1)}{2[1 + I_1(\mu_r - 1)]} \\ &\quad \times |\mathbf{h}^e|^2 \mu_0 |\Omega|, \end{aligned} \quad (11)$$

where  $|\Omega| = 4\pi a^2 c/3$  is the volume of the spheroid,  $|\partial\Omega| = 2\pi a^2 [1 + \frac{c}{ae} \sin^{-1}(e)]$  for a prolate spheroid with  $c > a$ ,  $e = \sqrt{1 - \frac{a^2}{c^2}}$ , and  $I_1$  is termed the demagnetization factor and is given by Eq. (A8). To account for the volume constraint (5), we simply replace  $c$  by  $\frac{R_0^3}{a^2}$  in Eq. (11). To account for the constraint (4), the best-fitting spheroid in the equilibrium state can be found by the method of Lagrange multiplier [ $\bar{F}(a, \bar{t}, \lambda) := F(a, \bar{t}) - \lambda(\bar{t}|\partial\Omega| - t_0|\partial\Omega_0|)$ ], where  $|\partial\Omega_0| = 4\pi R_0^2$  is the

TABLE I. Numerical values used to generate all the results.

Quantities	Values
$\eta$	0.1
$\mu_0$ (N/A <sup>2</sup> )	$4\pi \times 10^{-7}$
$\kappa_r$ (N/m)	0.142 <sup>a</sup>
$\kappa_s$ (N/m)	0.106 <sup>b</sup>
$\epsilon_0$ (F/m)	$8.854 \times 10^{-12}$
$E_0 = -V_0/t_0$ (V/m)	10 <sup>7c</sup>
$\epsilon_r$	20 <sup>d</sup>
$t_0$ (nm)	5 <sup>e</sup>
$R_0$ ( $\mu$ m)	5 <sup>f</sup>

<sup>a</sup>Reference [45].

<sup>b</sup>Reference [46].

<sup>c</sup>Reference [47].

<sup>d</sup>Reference [48].

<sup>e</sup>Reference [49].

<sup>f</sup>Reference [50].

surface area of a sphere in the reference configuration

$$\frac{\partial \tilde{F}}{\partial a} = 0, \quad \frac{\partial \tilde{F}}{\partial \tilde{r}} = 0, \quad \frac{\partial \tilde{F}}{\partial \lambda} = 0. \quad (12)$$

With the previously stated assumptions, the minimization problem becomes algebraic; however, the ensuing set of equations cannot be explicitly solved. For given  $|\mathbf{h}^e|$ ,  $V_0$ ,  $\epsilon_r$ ,  $\mu_r$ ,  $\kappa_r$ ,  $\kappa_s$ ,  $t_0$ , and  $R_0$  (see Table I), we can numerically solve the system of equations and determine the change of electric field induced by an externally applied magnetic field.

(ii) Although the assumption that the change in thickness of the membrane is uniform yields a simple physical consequence (to be elaborated upon in due course), the reality is slightly more complex. If we consider the thickness deformation to constitute an infinite set of modes, a uniform change is merely the first one. However, the response of the cell should also depend on the polar angle. This requires at least accounting for the second admissible deformation mode that depends nontrivially on the polar angle. Based on symmetry analysis, the leading two modes of thickness deformation can be expressed as

$$t = t_1 + t_2 \cos^2 \theta \quad \text{on } \partial\Omega_0, \quad (13)$$

where  $t_1$  and  $t_2$  are constants (i.e., mode amplitudes). Accounting for Eq. (13), the minimization problem (10) leads to a yet more complicated set of nonlinear algebraic equations that must also be solved numerically (see details in the Appendix). The detailed results and implications will be presented and discussed in the next section.

### III. RESULTS AND DISCUSSION

The first of our central results is shown in Fig. 3. The change in electrical field of the cell when subjected to a magnetic field is plotted as a function of the cell's interior relative magnetic permeability. Figure 3 corresponds to the case where we consider only the first deformation mode, i.e., the change of cell membrane thickness change is uniform. We note the following remarkable result, which may be considered as one of the key highlights of this work: Even if the relative

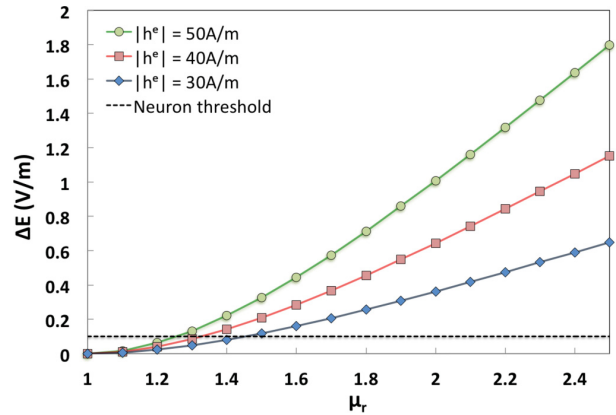


FIG. 3. Variation of the electric field within a cell membrane with respect to the relative permeability for different magnitudes of the Earth's magnetic field. To make quantitative estimates, we consider a cell subjected to a magnetic field and plot the ensuing change in the electrical field  $\Delta E$  as a function of the magnetic permeability of its interior. For example, a neuron can sense a variation in electric field as low as 0.1 V/m; the dashed line shows this threshold. These calculations are done using (14) under the assumption that the thickness across the membrane remains uniform.

magnetic permeability of the biological cell is only slightly higher than in vacuum, the cell behaves like a magnetoelectric material and can convert magnetic signals into electrical ones within the detectable range of biological cells.

A relative permeability of the cell interior that is greater than that of vacuum may be explained by the presence of magnetites (iron oxides) within the cytoplasm or any other number of reasons. The key point is that as long as the relative magnetic permeability of the biological cell is larger than that of the vacuum, the cell behaves like a magnetoelectric material and its ability to convert magnetic signals into electrical ones depends on both the precise value of the permeability and the strength of the applied field. Our proposed mechanism is complementary to the experimental works [32,33,35,36] that have detected magnetites in cells of certain animals (however, our model precisely explains how magnetic signals are converted into electrical ones). Further, the model we have put forward works equally well for both aquatic and land-based animals. Its practical feasibility is evident by the fact that relatively little is required for a cell interior to possess a magnetic permeability greater than one. In fact, just a small amount of magnetites will lead to this condition. The precise value of the relative magnetic permeability  $\mu_r$  of magnetite (as found in the biological context) is not known; however, it is expected to be of the order of 10 [53]. Using the Hashin-Strikmann bounds [54,55], we can deduce that less than 15.6% of magnetite particles are needed to realize an overall  $\mu_r$  of 1.4, sufficient for our proposed mechanism to be feasible (as is evident from Fig. 3). We can provide further confidence in this estimate by noting that in a recent experimental work [56], Rahmani shows that a monodispersed ferrofluid with 15-nm magnetite particles was seen to possess an overall relative magnetic permeability of 1.27 at 5 vol % fraction.



FIG. 4. Schematic of a magnetic map. The isolines represent isodynamics (lines of equal magnetic field intensity) with a contour interval equal to 4 A/m.

As shown in Fig. 4, the geomagnetic field is not constant and its magnitude on the Earth's surface ranges from 20 to 50 A/m. As the animals travel across many isodynamic lines, the magnetoelectric effect within a cell membrane will also vary, leading to a change in the electric field across the membrane. The change of electric field  $\Delta E$  in the presence of an external magnetic field is appropriate for evaluating the strength of this magnetoelectric coupling. By definition, the change of electric field  $\Delta E$  after and before application of external magnetic field is given by

$$\Delta E = E'_0 \left( \frac{\bar{t}'}{t|_{\mathbf{h}^e \neq 0}} - 1 \right), \quad (14)$$

where  $\bar{t}'$  is the equilibrium thickness when  $\mathbf{h}^e = 0$  and  $E'_0 = V_0/\bar{t}'$  ( $V_0$  is the transmembrane potential). The change in the electric field can be measured as if the animals make a differential comparison between two cells: one with magnetites in its interior (and hence a nontrivial magnetic permeability greater than the vacuum) and the other with a conventional magnetic permeability of the vacuum. Experiments have shown that an electric field as weak as 0.1 V/m is sensed by neurons and can modulate neuronal activity [57]. We also remark here that the minimum electrical activity that can be detected by a biological cell has been an area of active research (see [58–60]). Several theoretical models predict threshold sensitivity of living cells with order of magnitudes less than 0.1 V/m for both dc electric fields in the case of animals such as sharks (see Table 1 of Ref. [58]) and for weak and extremely-low-frequency electric fields [59]. Due to the lack of experimental work for dc fields, we have chosen the threshold 0.1 V/m for reference. Animals, by varying their positions, generate different electric responses recognized by their neuronal or cellular systems that (we believe) help them distinguish positional information and thus assess their geographical locations as shown in Figs. 3 and 4. Here we remark that the voltage drop across the entire cell is quite different than across the membrane and the reader should exercise care in comparing such values across our paper and other works, e.g., [58]; further details on this matter are discussed by Ahmadpour *et al.* [60].

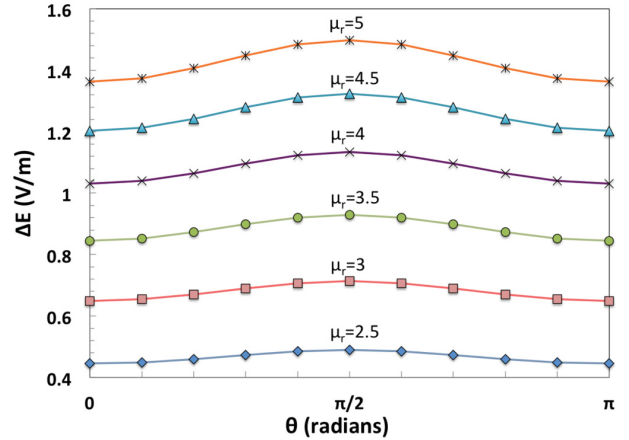


FIG. 5. Variation of the electric field within a cell membrane for a fixed value of the Earth's magnetic field. We consider  $|h^e| = 50$  A/m and plot the change in the electrical field as a function of the polar angle  $\theta$  for several values of the magnetic permeability. Evidently, a local change in the animal position by a simple rotation produces a change in the resulting electric field. These calculations are done using (14) under the assumption (13).

While the magnetic-map ability can be explained by assuming the first thickness deformation mode, i.e., a uniform thinning of the membrane (as elaborated in the previous paragraphs), the mystery behind the compass ability can only be elucidated by invoking the polar angle dependence of the local thickness of the membrane  $t$  and the change of the membrane electric field  $\Delta E$ . Figures 5 and 6 reveal why we must consider the second mode in Eq. (13) to explain the compass ability. Why does this matter so much? To answer this question let us first recall that the magnetic lines leave the southern hemisphere and enter the northern hemisphere.

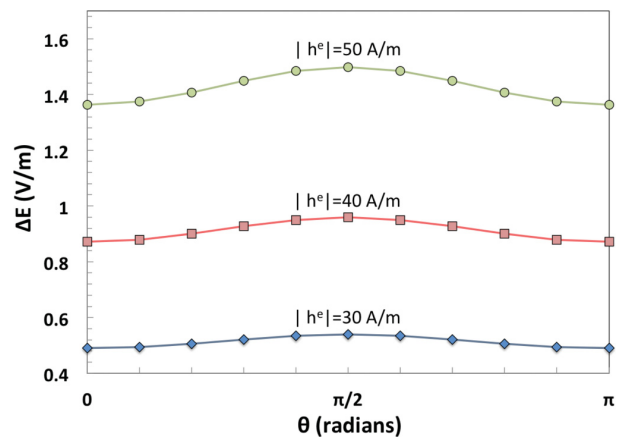


FIG. 6. Variation of the electric field within a cell membrane for a fixed value of the relative permeability of its interior. We consider  $\mu_r = 5$  and plot the ensuing change in the electrical field as a function of the polar angle  $\theta$  for several values of the geomagnetic field. As is evident, the animal captures the intensity of the magnetic field and recognizes locally a sense of its direction. These calculations are done using (14) under the assumption (13).

When subjected to the geomagnetic field, the cell deforms into a prolate ellipsoid and like a compass needle will tend to align itself with respect to the magnetic line. By including the second mode, the thickness will change with respect to the polar angle, i.e., the cell will have different thicknesses across the polar axis and the equator axis. As a result, by turning its body and interrogating the electric field change at a fixed position, the animal will achieve a sense of direction. From symmetry arguments, we can also infer that the animal cannot differentiate between north and south or east and west based on this mechanism. This has also been previously noted by Shcherbakov and Winklhofer [23].

Our arguments thus far are enough to explain why some animals like European robins have the so-called inclination compass ability allowing them to be sensitive to the field's axis but not to its polarity [8]. Instead it relies on the magnetic inclination, which is the angle measured between the horizontal axis and the Earth's magnetic field lines. In fact, the horizontal surface crossing through the cell is somehow a reference surface and will have an electric print that will adjust as the angle with the Earth's surface changes [Fig. 7(a)].

Another way to approach the aforementioned problem is to break the mirror symmetry by assuming that the relative permeability  $\mu_r(\mathbf{r})$  is nonuniformly distributed inside the cell and thus depends on the position vector. The underlying hypothesis is that the small iron-oxide magnetite crystals inside a cell will align themselves along with the geomagnetic line. The force between the particles will exert pressure on the membrane, imposing an additional thinning on one particular pole [Fig. 7(b)]. In such a case, the animal will have the ability to distinguish between all the directions. However, we recognize that only a minority of the magnetosensitive animals appear to be able to detect the polarity of the Earth's magnetic field and thus distinguish between north and south (e.g., lobsters, salamanders, and mole rats) [14]. In any event, we do not explore this possibility in the present work as we lack sufficient experimental cues to justify such an effort. In

particular, we have avoided that calculation to avoid detracting from our central message.

In summary, we are able to outline a rather simple and robust mechanism that appears to quantitatively explain most of the experimental observations pertaining to magnetoreception in animals. The key notion is that nonlinear elastic deformation must be properly accounted for. Then, as long as there exists a preexisting voltage across the cell membrane (which is nearly always true) and the magnetic permeability of the cell interior is greater than that of a vacuum, all biological cells become capable of detecting the magnetic field. The strength of this coupling depends on the precise value of the magnetic permeability of the cell. The higher the value, the better the resolution and ability of the animal. We note that the enhanced magnetic permeability is easily achieved by even minuscule amounts of magnetic particles that have been experimentally detected in magnetosensitive animals. For the typical value of the Earth's magnetic field, the neuronal or cellular sensitivity threshold of 0.1 V/m is easily exceeded for even moderate values of magnetic permeabilities (Fig. 8). An aspect that may need further elaboration is that we have treated intracellular and extracellular media as fluids and have neglected any elastic contribution. While we believe that this assumption is well justified, further consideration regarding the mechanical properties of cell interior and exterior is a worthwhile undertaking [61]. Our consideration of surface elasticity is primarily informed by the studies concluding that cell surface mechanics dictates cell morphology [62,63]. Furthermore, we expect similar strain-mediated magnetoelectricity to occur as long as the surrounding (and interior) cellular material is very compliant.

ACKNOWLEDGMENTS

S.K. and P.S. gratefully acknowledge the financial support from the M. D. Anderson Professorship. L.L. gratefully acknowledges the support of NSF Grants No. CMMI-135156, No. DMS-1410273, and No. AFOSR-FA9550-16-1-0181.

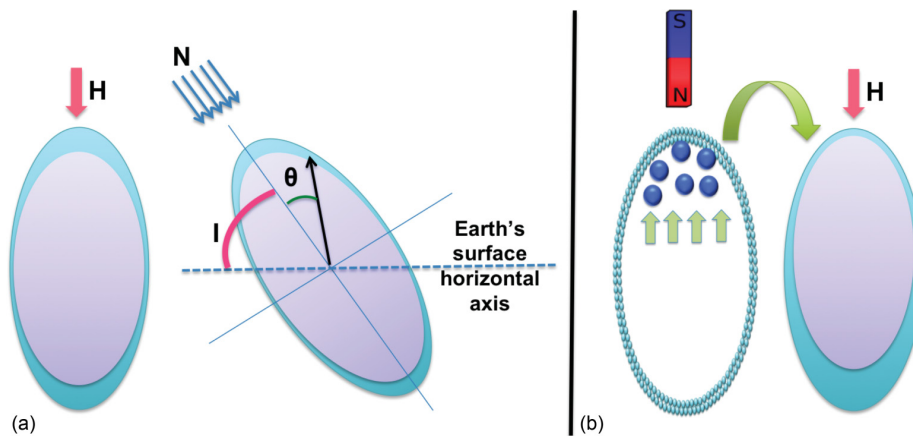


FIG. 7. Schematic of the possible ways to include the compass ability in the presented mechanism. (a) Adding a correction mode to the thickness (the inclination angle  $I$  is the angle measured between the Earth's surface and the geomagnetic lines and  $\theta$  is the polar angle within the spheroidal coordinates system and belongs to  $[0, \pi]$ ). (b) Introduction of a nonuniformly distributed relative permeability inside the cell caused by the concentration of magnetites in a specific region.

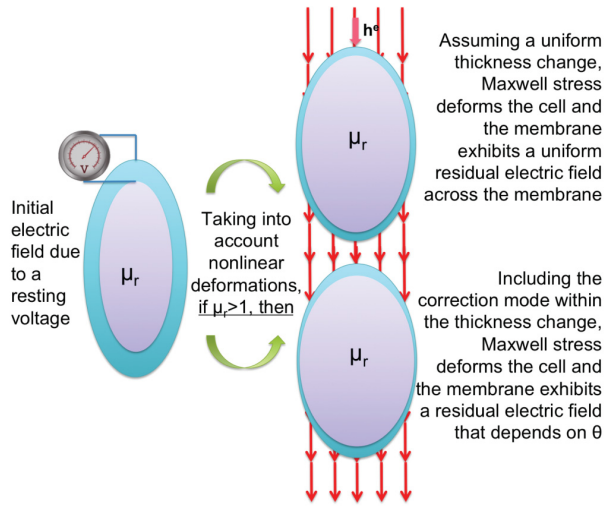


FIG. 8. Key ingredients of the mechanism underlying the conversion of magnetic signal into a change in electrical field and its relation to thickness and  $\theta$ .

### APPENDIX

In this Appendix we highlight the various details related to the mathematical calculations. The geometrical deformation that the cell undergoes upon exposure to higher<sup>4</sup> magnetic fields is shown in Fig. 9. We also illustrate the variation of

<sup>4</sup>Relatively higher, since for very high magnetic fields, instability may ensue, which is not accounted for in our model.

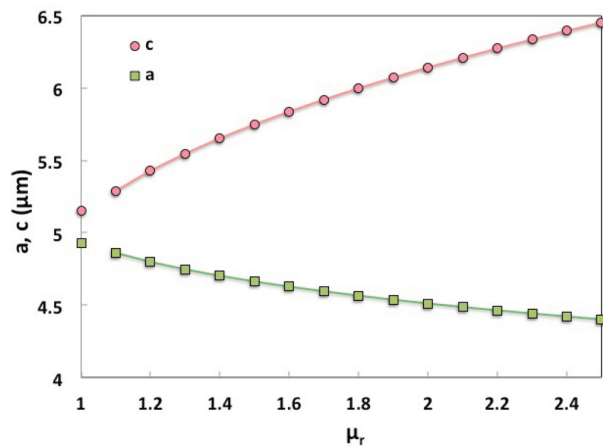


FIG. 9. Deformation of the ellipsoid's equator and polar semiaxis ( $a$  and  $c$ ) with respect to the relative magnetic permeability of the interior of the cell. As is evident, if the relative permeability  $\mu_r = 1$  then there is no effect of the magnetic field on the biological cell. In that case, only the transmembrane voltage will deform its shape. The data points corresponding to  $\mu_r = 1$  show the equilibrium state of the cell when the magnetic field is switched off. However, when  $\mu_r > 1$ , the cell becomes magnetosensitive and deforms further. ( $|h^e| = 50$  kA/m.)

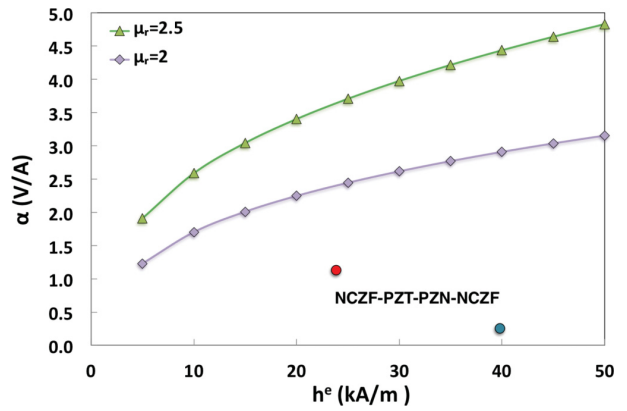


FIG. 10. Magnetolectric coupling constants at high external magnetic field. The colored lines show the coupling constant of a biological membrane. The data points displays the magnetolectric coefficient of the NCZF-PZT-PZN-NCZF composite.

the magnetolectric coupling constant and the thinning of the membrane for higher external magnetic fields in Figs. 10 and 11, respectively.

#### 1. Elastic contribution

The elastic energy is given by Eq. (3). When  $t = \bar{t} = \text{const}$ , the elastic energy can be expressed as

$$U_{\text{elast}}[\mathbf{y}] = \frac{\pi \kappa_s}{2R_0^2} \left[ a^2 \left( \frac{c \sin^{-1}(e)}{ae} + 1 \right) - 2R_0^2 \right]^2 + \pi a^2 \left( \frac{t}{t_0} - 1 \right)^2 \kappa_t \left( \frac{c \sin^{-1}(e)}{ae} + 1 \right). \quad (\text{A1})$$

If the second deformation mode is considered, the first term of Eq. (3) should be evaluated again over the surface of the prolate ellipsoid by replacing  $t = t_1(1 + \eta \cos^2 \theta)$  with  $\eta = t_2/t_1$ .

In addition, our elastic model assumes incompressibility of the cell membrane, which implies Eq. (4). For the uniform

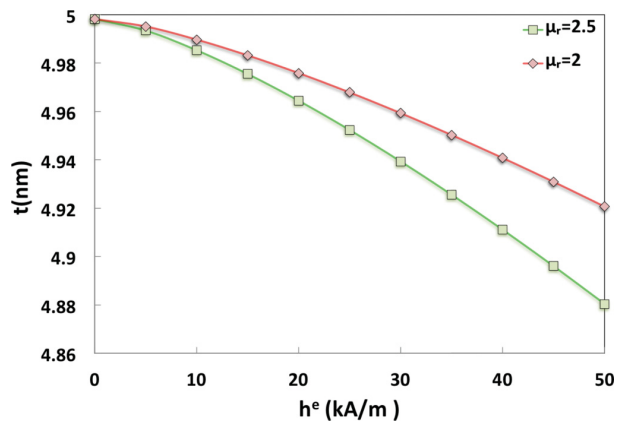


FIG. 11. Dependence of the membrane's uniform thickness on the external magnetic field intensity. At a high external magnetic field intensity, the thinning on the membrane is more important. It becomes more pronounced as we keep increasing the intensity.

thickness  $t = \bar{t} = \text{const}$ , Eq. (4) can be rewritten as

$$\mathcal{I}_1[\mathbf{y}] = 2\pi \left( \frac{ac\bar{t} \sin^{-1}(e)}{e} + a^2\bar{t} - 2R_0^2 t_0 \right). \quad (\text{A2})$$

If  $t = t_1(1 + \eta \cos^2 \theta)$ ,

$$\begin{aligned} \mathcal{I}_1[\mathbf{y}] = & \frac{\pi a t_1}{2c^2 e^3} \left[ [c^3(\eta + 4) - 4a^2 c] \tan^{-1} \left( \frac{ce}{a} \right) \right. \\ & \left. + ae[c^2(\eta + 4) - 2a^2(\eta + 2)] \right] - 4\pi R_0^2 t_0. \quad (\text{A3}) \end{aligned}$$

## 2. Electric contribution

In the following, we show detailed calculations of the electric contribution to the total free energy. First, by definition, the electric contribution is given by Eq. (6) and can be rewritten as

$$\mathcal{E}_{\text{elct}}[\Omega, \mathbf{p}; V_0] = -\frac{\epsilon_0 \epsilon_r}{2} \int_{\mathcal{M}} |\nabla \varphi|^2. \quad (\text{A4})$$

To see this, by the divergence theorem we have the identity

$$\begin{aligned} & \int_{\partial \mathcal{M}} \varphi (-\epsilon_0 \nabla \varphi + \mathbf{p}) \cdot \mathbf{n} \\ &= \int_{\mathcal{M}} \nabla \cdot [\varphi (-\epsilon_0 \nabla \varphi + \mathbf{p})] \\ &= \int_{\mathcal{M}} \nabla \varphi \cdot (-\epsilon_0 \nabla \varphi + \mathbf{p}) + \int_{\mathcal{M}} \varphi \nabla \cdot (-\epsilon_0 \nabla \varphi + \mathbf{p}), \end{aligned}$$

where the last equality follows from the Maxwell equation (7). Applying the constitutive law  $\mathbf{p} = -\epsilon_0(\epsilon_r - 1)\nabla \varphi$ , by Eq. (6) we obtain

$$\begin{aligned} \mathcal{E}_{\text{elct}}[\Omega, \mathbf{p}; V_0] &= \int_{\mathcal{M}} \frac{|-\epsilon_0(\epsilon_r - 1)\nabla \varphi|^2}{2\epsilon_0(\epsilon_r - 1)} + \frac{\epsilon_0}{2} \int_{\mathcal{M}} |\nabla \varphi|^2 \\ &+ \int_{\mathcal{M}} \nabla \varphi \cdot [-\epsilon_0 \nabla \varphi - \epsilon_0(\epsilon_r - 1)\nabla \varphi] \\ &= -\frac{\epsilon_0 \epsilon_r}{2} \int_{\mathcal{M}} |\nabla \varphi|^2. \end{aligned}$$

Moreover, since the radius of the cell is much greater than the membrane thickness  $R_0 \gg t$ , the solution to the Maxwell equation (7) and Eq. (1) is approximately given by

$$-\nabla \varphi \approx -\frac{V_0}{t} \mathbf{e}_r \quad \text{on } \mathcal{M}. \quad (\text{A5})$$

When  $t = \bar{t}$ , the electric contribution becomes

$$\mathcal{E}_{\text{elct}} = -\frac{\pi a^2 E_0^2 t_0^2 \epsilon_0 \epsilon_r}{\bar{t}} \left( 1 + \frac{c \sin^{-1}(e)}{ae} \right). \quad (\text{A6})$$

If the second deformation mode is considered, we need to substitute  $t = t_1(1 + \eta \cos^2 \theta)$  into (A5) and reevaluate the expression of the integral (A4).

## 3. Magnetic contribution

As is well known, a uniformly magnetized ellipsoid induces a uniform magnetic field inside the ellipsoid, i.e., the solution to Eq. (9) for constant  $\mathbf{m} \in \mathbb{R}^3$  satisfies

$$\nabla \xi = \mathbf{Qm} \quad \text{in } \Omega, \quad (\text{A7})$$

where  $\mathbf{Q} = \text{diag}[I_1, I_2, I_3]$  with the demagnetization factors  $I_i$  that are determined by the shape of the ellipsoid

$$I_1 = 1 - 2I_2, \quad I_2 = \frac{a^2 c}{2} \int_0^\infty \frac{1}{(a^2 + u)^2 \sqrt{c^2 + u}} du. \quad (\text{A8})$$

In addition, by the divergence theorem and Eq. (9) we have

$$0 = \int_{\mathbb{R}^3} \nabla \xi \cdot (-\nabla \xi + \mathbf{m} \chi_\Omega) = \int_{\mathbb{R}^3} |\nabla \xi|^2 - \int_{\mathbb{R}^3} \nabla \xi \cdot \mathbf{m} \chi_\Omega \quad (\text{A9})$$

and hence

$$\frac{\mu_0}{2} \int_{\mathbb{R}^3} |\nabla \xi|^2 = \frac{\mu_0}{2} \int_{\mathbb{R}^3} \nabla \xi \cdot \mathbf{m} \chi_\Omega = \frac{\mu_0}{2} |\Omega| \mathbf{m} \cdot \mathbf{Qm}. \quad (\text{A10})$$

Therefore, the magnetic contribution to the total free energy as defined by Eq. (8) is given by

$$\begin{aligned} \mathcal{E}_{\text{mag}}[\Omega, \mathbf{m}] &= -\frac{\mu_r - 1}{2[1 + I_1(\mu_r - 1)]} |\mathbf{h}^\ell|^2 \mu_0 |\Omega| \\ &= -\frac{2\pi a^2 c |\mathbf{h}^\ell|^2 \mu_0 (\mu_r - 1)}{3 \left( 1 + \frac{a^2(\mu_r - 1)(-ace \cos^{-1}(\frac{c}{a}) + a^2 - c^2)}{(a^2 - c^2)^2} \right)}. \quad (\text{A11}) \end{aligned}$$

We remark that the magnetic energy does not depend on the thickness of the membrane.

## 4. Ellipsoidal shape and dimensions change

In this section we investigate the deformation that a cell undergoes under a high magnetic field if a uniform thickness of the cell membrane is assumed. The starting configuration of the cell is considered to be a sphere of radius  $5 \mu\text{m}$  with membrane thickness of  $5 \text{ nm}$ . A typical cell membrane has a nominal electric field of the order of  $10^7 \text{ V/m}$  across the membrane due to an ion imbalance of actively gated transportation. By introducing this transmembrane potential and subjecting the cell to the magnetic field, the Maxwell stress will impact the elastic state of the cell by deforming its configuration to an ellipsoid. From Fig. 9 we can observe the equilibrium values of the ellipsoid's equator and polar semiaxis ( $a$  and  $c$ ) with respect to the relative permeability.

A few remarks regarding the extent of the deformation and thermal fluctuations are in order. Due to the preexisting electric field, the initial configuration of the cell corresponds to  $a/c = 0.94$ . For a typical terrestrial magnetic field (and at a cell magnetic permeability of 1.1) the cell will be further deformed to  $a/c = 0.92$ . For a magnetic permeability of 2.5, this changes to 0.68. At physiological temperatures, cell membranes do undulate noticeably. However, thermal fluctuations are not symmetry breaking, so their mean aspect ratio does not change as a result. A proper statistical mechanics analysis is in fact nontrivial due to the highly nonlinear coupling inherent in our model. We defer a full analysis of this aspect to future work. Meanwhile, we simply point out that to a first order, thermal fluctuations are only expected to improve the sensitivity of the conversion of magnetic field into electric signals. As is well known, thermal fluctuations cause softening of membrane mechanical properties (see, e.g., [64]). A decrease in stretch modulus will increase the deformation and hence likely increase the sensitivity of the magnetic to electric conversion.

Finally, Bacri *et al.* [65] have experimentally confirmed that magnetic fields tend to suppress thermal fluctuations.

The terrestrial magnetic field is rather small, so the issue of the maximum magnetoelectric coupling becomes somewhat moot but is of course relevant under other contexts, e.g., animals subject to artificially created high fields or design of soft artificial magnetoelectric composites. We believe that if the magnetic field is increased excessively, at some point, the vesicle or membrane will exhibit an electromagnetic instability, as is often observed in soft materials. The detailed answer to this issue however requires an in-depth stability and bifurcation analysis, which is beyond the scope of this paper.

### 5. High external magnetic field

By determining the change of the transmembrane electric field induced by the external magnetic field, we can determine the dependence of the magnetoelectric coupling constant  $\alpha = \frac{\Delta E}{|h^c|}$  on the external magnetic field intensity under the

assumption of a uniform thickness. In the presence of a high external magnetic field, the magnetoelectric coefficient of the membrane within an animal cell displays values comparable to some well-known artificial magnetoelectric composites as shown in Fig. 10. At a field strength of 23.8 kA/m, the trilayer composite NCZF-PZT-PZN-NCZF has an  $\alpha$  of 1.13 V/A [66]. For this same external field, the magnetoelectric coefficient across a biomembrane is around 2.4 V/A when the relative permeability  $\mu_r = 2$  and almost 3.6 V/A when  $\mu_r = 2.5$ . The  $\alpha$  of the trilayer composite drops to 0.25 V/A at a field strength of 40 kA/m [66], but increases in the case of the biological bilayer reaching 2.9 V/A when  $\mu_r = 2$  and 4.4 V/A when  $\mu_r = 2.5$  at the same field intensity. When subjected to a relatively high external field, the biomembrane is polarized and the thinning caused by Maxwell stress is more pronounced. The concentration of magnetites inside the cell contributes in the polarization process: The higher the relative permeability of the cell interior, the more compressed the membrane (Fig. 11).

- 
- [1] R. Blakemore, Magnetotactic bacteria, *Science* **190**, 377 (1975).
- [2] K. J. Lohmann, Magnetic orientation by hatchling loggerhead sea turtles (*Caretta caretta*), *J. Exp. Biol.* **155**, 37 (1991).
- [3] L. Q. Wu and J. D. Dickman, Neural correlates of a magnetic sense, *Science* **336**, 1054 (2012).
- [4] P. O'Neill, Magnetoreception and baroreception in birds, *Dev., Growth & Differentiation* **55**, 188 (2013).
- [5] S. Johnsen and K. J. Lohmann, The physics and neurobiology of magnetoreception, *Nat. Rev. Neurosci.* **6**, 703 (2005).
- [6] R. Wiltschko and W. Wiltschko, *Magnetic Orientation in Animals* (Springer, Berlin, 1995).
- [7] W. Wiltschko and R. Wiltschko, Magnetic orientation and magnetoreception in birds and other animals, *J. Comp. Physiol. A* **191**, 675 (2005).
- [8] W. Wiltschko and R. Wiltschko, Magnetic compass of European robins, *Science* **176**, 62 (1972).
- [9] R. Wiltschko and W. Wiltschko, Avian navigation: From historical to modern concepts, *Anim. Behav.* **65**, 257 (2003).
- [10] K. J. Lohmann and C. M. F. Lohmann, Sea turtles, lobsters, and oceanic magnetic maps, *Mar. Freshwater Behav. Physiol.* **39**, 49 (2006).
- [11] K. J. Lohmann, Magnetic-field perception, *Nature (London)* **464**, 1140 (2010).
- [12] K. J. Lohmann, C. M. F. Lohmann, and N. F. Putman, Magnetic maps in animals: Nature's GPS, *J. Exp. Biol.* **210**, 3697 (2007).
- [13] D. D. Skiles, *Magnetite Biomineralization and Magnetoreception in Organisms* (Springer, New York, 1985), pp. 43–102.
- [14] S. Johnsen and K. J. Lohmann, Magnetoreception in animals, *Phys. Today* **61**(3), 29 (2008).
- [15] M. Winklhofer and J. L. Kirschvink, A quantitative assessment of torque-transducer models for magnetoreception, *J. R. Soc. Interface* **7**, 273 (2010).
- [16] P. J. Hore and H. Mouritsen, The radical-pair mechanism of magnetoreception, *Annu. Rev. Biophys.* **45**, 299 (2016).
- [17] I. A. Solov'yov, P. J. Hore, T. Ritz, and K. Schulten, in *Quantum Effects in Biology*, edited by M. Mohseni, Y. Omar, G. S. Engel, and M. B. Plenio (Cambridge University Press, Cambridge, 2014), pp. 218–236.
- [18] I. A. Solov'yov, T. Domratcheva, and K. Schulten, Separation of photo-induced radical pair in cryptochrome to a functionally critical distance, *Sci. Rep.* **4**, 3845 (2014).
- [19] I. A. Solov'yov, H. Mouritsen, and K. Schulten, Acuity of a cryptochrome and vision based magnetoreception system in birds, *Biophys. J.* **99**, 40 (2010).
- [20] H. Mouritsen and T. Ritz, Magnetoreception and its use in bird navigation, *Curr. Opin. Neurobiol.* **15**, 406 (2005).
- [21] T. Ritz, D. H. Dommer, and J. B. Phillips, Shedding light on vertebrate magnetoreception, *Neuron* **34**, 503 (2002).
- [22] D. T. Edmonds, A sensitive optically detected magnetic compass for animals, *Proc. R. Soc. London* **263**, 295 (1996).
- [23] V. P. Shcherbakov and M. Winklhofer, The osmotic magnetometer: A new model for a magnetite-based magnetoreceptor in animals, *Eur. Biophys. J.* **28**, 380 (1999).
- [24] J. L. Kirschvink and J. L. Gould, Biogenic magnetite as a basis for magnetic field detection in animals, *BioSystems* **13**, 181 (1981).
- [25] T. Ritz, S. Adem, and K. Schulten, A model for photoreceptor-based magnetoreception in birds, *Biophys. J.* **78**, 707 (2000).
- [26] K. Wang, E. Mattern, and T. Ritz, On the use of magnets to disrupt the physiological compass of birds, *Phys. Biol.* **3**, 220 (2006).
- [27] C. T. Rodgers and P. J. Hore, Chemical magnetoreception in birds: The radical pair mechanism, *Proc. Natl. Acad. Sci. USA* **106**, 353 (2009).
- [28] T. Ritz, R. Wiltschko, P. J. Hore, C. T. Rodgers, K. Stapput, P. Thalau, C. R. Timmel, and W. Wiltschko, Magnetic compass of birds is based on a molecule with optimal directional sensitivity, *Biophys. J.* **96**, 3451 (2009).
- [29] T. Ritz, M. Ahmad, H. Mouritsen, R. Wiltschko, and W. Wiltschko, Photoreceptor-based magnetoreception: Optimal design of receptor molecules, cells, and neuronal processing, *J. R. Soc. Interface* **7**, S135 (2010).

- [30] A. J. Kalmijn, The detection of electric fields from inanimate and animate sources other than electric organs, in *Electroreceptors and Other Specialized Receptors in Lower Vertebrates*, edited by A. Fessard, Handbook of Sensory Physiology Vol. 3 (Springer, Berlin, Heidelberg, 1974), pp. 147–200.
- [31] K. J. Lohmann and S. Johnsen, The neurobiology of magnetoreception in vertebrate animals, *Trends Neurosci.* **23**, 153 (2000).
- [32] M. M. Walker, C. E. Diebel, C. V. Haugh, P. M. Pankhurst, J. C. Montgomery, and C. R. Green, Structure and function of the vertebrate magnetic sense, *Nature (London)* **390**, 371 (1997).
- [33] C. E. Diebel, R. Proksch, C. R. Green, P. Neilson, and M. M. Walker, Magnetite defines a vertebrate magnetoreceptor, *Nature (London)* **406**, 299 (2000).
- [34] I. A. Solov'yov and W. Greiner, Micromagnetic insight into a magnetoreceptor in birds: Existence of magnetic field amplifiers in the beak, *Phys. Rev. E* **80**, 041919 (2009).
- [35] G. Fleissner, E. Holtkamp-Rotzler, M. Hanzlik, M. Winklhofer, G. Fleissner, N. Petersen, and W. Wiltchko, Ultrastructural analysis of a putative magnetoreceptor in the beak of homing pigeons, *J. Comp. Neurol.* **458**, 350 (2003).
- [36] M. Winklhofer, E. Holtkamp-Rotzler, M. Hanzlik, G. Fleissner, and N. Petersen, Clusters of superparamagnetic magnetite particles in the upper-beak skin of homing pigeons: Evidence of a magnetoreceptor? *Eur. J. Mineral.* **13**, 659 (2001).
- [37] C. D. Treiber, M. C. Salzer, J. Riegler, N. Edelman, C. Sugar, M. Breuss, P. Pichler, H. Cadiou, M. Saunders, M. Lythgoe, J. Shaw, and D. A. Keays, Clusters of iron-rich cells in the upper beak of pigeons are macrophages not magnetosensitive neurons, *Nature (London)* **484**, 367 (2012).
- [38] C. D. Treiber, M. Salzer, M. Breuss, L. Ushakova, M. Lauwers, N. Edelman, and D. A. Keays, High resolution anatomical mapping confirms the absence of a magnetic sense system in the rostral upper beak of pigeons, *Commun. Integr. Biol.* **6**, e24859 (2013).
- [39] K. Maeda, K. B. Henbest, F. Cintolesi, I. Kuprov, C. T. Rodgers, P. A. Liddell, D. Gust, C. R. Timmel, and P. J. Hore, Chemical compass model of avian magnetoreception, *Nature (London)* **453**, 387 (2008).
- [40] A. P. Pyatakov and A. K. Zvezdin, Magnetolectric and multiferroic media, *Phys. Usp.* **55**, 557 (2012).
- [41] J. P. Velev, S. S. Jaswal, and E. Y. Tsymbal, Multiferroic and magnetolectric materials and interfaces, *Philos. Trans. R. Soc. A* **369**, 3069 (2011).
- [42] J. F. Scott, Applications of modern ferroelectrics, *Science* **315**, 954 (2007).
- [43] L. Liu and P. Sharma, Giant and universal magnetolectric coupling in soft materials and concomitant ramifications for materials science and biology, *Phys. Rev. E* **88**, 040601(R) (2013).
- [44] J. C. Maxwell, *A Treatise on Electricity and Magnetism* (Clarendon, Oxford, 1873).
- [45] C. Nielsen, M. Goulian, and O. S. Andersen, Energetics of inclusion-induced bilayer deformations, *Biophys. J.* **74**, 1966 (1998).
- [46] L. Picas, F. Rico, and S. Scheuring, Direct measurement of the mechanical properties of lipid phases in supported bilayers, *Biophys. J.* **102**, L01 (2012).
- [47] D. A. McCormick, *From Molecules to Networks*, 3rd ed. (Academic, Boston, 2014), pp. 351–376.
- [48] H. A. Stern and S. E. Feller, Calculation of the dielectric permittivity profile for a nonuniform system: Application to a lipid bilayer simulation, *J. Chem. Phys.* **118**, 3401 (2003).
- [49] B. Alberts, A. Johnson, J. Lewis, D. Morgan, M. Raff, K. Roberts, and P. Walter, *Molecular Biology of the Cell*, 5th ed. (Garland Science, New York, 2014), pp. 617–650.
- [50] B. Alberts, A. Johnson, J. Lewis, D. Morgan, M. Raff, K. Roberts, and P. Walter, *Molecular Biology of the Cell* (Ref. [49]), pp. 579–615.
- [51] L. Liu, An energy formulation of continuum magneto-electroelasticity with applications, *J. Mech. Phys. Solids* **63**, 451 (2014).
- [52] L. Liu, On energy formulations of electrostatics for continuum media, *J. Mech. Phys. Solids* **61**, 968 (2013).
- [53] V. P. Shcherbakov and M. Winklhofer, Theoretical analysis of flux amplification by soft magnetic material in a putative biological magnetic-field receptor, *Phys. Rev. E* **81**, 031921 (2010).
- [54] L. Liu, Effective conductivities of two-phase composites with a singular phase, *J. Appl. Phys.* **105**, 103503 (2009).
- [55] Z. Hashin and S. Shtrikman, A variational approach to the theory of the effective magnetic permeability of multiphase materials, *J. Appl. Phys.* **33**, 3125 (1962).
- [56] A. R. Rahmani, Modeling of recovery process characterization using magnetic nanoparticles, Ph.D. thesis, University of Texas, 2013, p. 138, Table 3.11.
- [57] J. T. Francis, B. J. Gluckman, and S. J. Schiff, Sensitivity of neurons to weak electric fields, *J. Neurosci.* **23**, 7255 (2003).
- [58] J. C. Weaver and R. D. Astumian, The response of living cells to very weak electric fields: The thermal noise limit, *Science* **247**, 459 (1990).
- [59] J. C. Weaver, T. E. Vaughan, R. K. Adair, and R. D. Astumian, Theoretical limits on the threshold for the response of long cells to weak extremely low frequency electric fields due to ionic and molecular flux rectification, *Biophys. J.* **75**, 2251 (1998).
- [60] F. Ahmadpoor, L. Liu, and P. Sharma, Thermal fluctuations and the minimum electrical field that can be detected by a biological membrane, *J. Mech. Phys. Solids* **78**, 110 (2015).
- [61] B. Fabry, G. N. Maksym, J. P. Butler, M. Glogauer, D. Navajas, and J. J. Fredberg, Scaling the Microrheology of Living Cells, *Phys. Rev. Lett.* **87**, 148102 (2001).
- [62] T. Lecuit and P. F. Lenne, Cell surface mechanics and the control of cell shape, tissue patterns and morphogenesis, *Nat. Rev. Mol. Cell Biol.* **8**, 633 (2007).
- [63] T. Hayashi and R. W. Carthew, Surface mechanics mediate pattern formation in the developing retina, *Nature (London)* **431**, 647 (2004).
- [64] L. Liu and P. Sharma, Flexoelectricity and thermal fluctuations of lipid bilayer membranes: Renormalization of flexoelectric, dielectric, and elastic properties, *Phys. Rev. E* **87**, 032715 (2013).
- [65] J. C. Bacri, V. Cabuil, A. Cebers, C. Menager, and R. Perzynski, Flattening of ferro-vesicle undulations under a magnetic field, *Europhys. Lett.* **33**, 235 (1996).
- [66] R. A. Islam and S. Priya, Progress in dual (piezoelectric-magnetostrictive) phase magnetolectric sintered composite, *Adv. Condens. Matter Phys.* **2012**, 320612 (2012).